Available online at www.sciencedirect.com
ScienceDirect
Ceramics International 36 (2010) 1951–1959
CERAMICS INTERNATIONAL
www.elsevier.com/locate/ceramint

Thermal conductivity of traditional ceramics. Part I: Influence of bulk density and firing temperature

J. García Ten *, M.J. Orts, A. Saburit, G. Silva

Instituto de Tecnología Cerámica, Asociación de Investigación de las Industrias Cerámicas, Universitat Jaume I, Campus Universitario Riu Sec, 12006 Castellón, Spain

Received 22 January 2010; received in revised form 17 March 2010; accepted 14 April 2010
Available online 11 June 2010

Abstract

The thermal conductivity of traditional ceramics is known to be a function of their porosity or bulk density. However, the scatter in the thermal conductivity–bulk density data in certain studies, particularly when data from industrially processed brick are involved, suggests that thermal conductivity depends, apart from porosity, on other characteristics such as phase composition, microstructure, humidity or the presence of soluble salts.

A red-firing clay used in brick manufacture has been used in this study with a view to systematising the impact of the different variables that could influence thermal conductivity and mechanical strength. This first paper presents the results obtained when the dry bulk density of the pieces and their firing temperature were modified.

It was confirmed that thermal conductivity did not solely depend on the total porosity of the fired pieces, but that pore size distribution and pore interconnectivity need to be considered, which depend on the degree of firing attained, and may also be influenced by the phases present in the pieces, whose content and/or composition could vary with firing temperature.

Keywords: C. Thermal conductivity; D. Clays; D. Traditional ceramics

1. Introduction

A key area in which energy consumption needs to be reduced is the thermal conditioning of dwellings and buildings, which requires improved thermal insulation of building envelopes. The entry into force of new European regulations has led to intense competition among the materials used in building envelopes, which might oust ceramic products, particularly in the colder regions. As a result, much attention has been paid in recent years to the thermal properties of traditional ceramic materials.

The thermal conductivity of ceramic materials is a function of their porosity or bulk density [1–3], and numerous studies have addressed the reduction of brick bulk density using lightening additives [4–6]. However, studies indicate that thermal conductivity does not depend exclusively on brick bulk density, but that other characteristics also significantly affect brick thermal conductivity, such as phase composition, microstructure, humidity or the presence of soluble salts [7–10].

The influence of these variables and the absence of systematic studies in the bibliography have led to a great scatter in the thermal conductivity–bulk density data in certain studies and models, particularly when data from industrially processed brick are involved [8,9,11]. In industrial brick manufacture, the differences in raw material mixtures and the manufacturing process used broaden the scatter of experimental data. Nevertheless, the use of statistical techniques allows certain conclusions to be drawn, such as the greater thermal conductivity of bricks that have high quartz and calcium crystalline phase contents [8,11].

When it is sought to decrease brick thermal conductivity by raising porosity, the ensuing reduction in mechanical strength needs to be taken into account, thus also making it of interest to understand how brick composition and microstructure influence mechanical strength [12,13]. This issue has been addressed in few studies, which report that the microstructures

* Corresponding author.
E-mail address: jgarcia@itc.uji.es (J. García Ten).

0272-8842/$36.00
doi:10.1016/j.ceramint.2010.05.012

formed by small pores provide greater mechanical strength [14].

With a view to systematising the study of the different variables that could influence thermal conductivity, is necessary first to establish the relationship between thermal conductivity and bulk density for the material under study, because the existing models do not predict the thermal conductivity with the required precision, due to the influence of other factors [7–10]. For this, the paper presents the results obtained when the dry bulk density of the materials and their firing temperature were modified.

2. Experimental

The study has been conducted with a red-firing clay (ref. IC produced by Caolines Lapiedra, S.L., Valencia, Spain) used in manufacturing tiles and bricks. Table 1 lists the chemical and mineralogical composition of the clay, which contains a mixture of clay minerals with an illitic–kaolinitic structure and an abundant quantity of quartz.

In order to prepare the test pieces, clay IC was dry milled in a hammer mill (Retch SKI), yielding a particle size fraction below 0.5 mm. The powder was then moistened to 0.055 kg water/dry solid kg and used to form two series of test pieces, referenced series 1 and series 2, by uniaxial pressing (Nanneti 15T Mignon). In series 1, the pressing pressure was varied between 10 and 60 MPa with a view to modifying the porosity of the green test pieces. These pieces were dried and then fired in an electric kiln (Pirometrol RAP100) at a heating rate of 5 °C/min. to a peak temperature of 1000 °C, with a 60-min dwell at peak temperature. Cooling was performed by natural convection. The series 2 pieces were pressed at constant pressure (25 MPa) and fired to different peak temperatures, between 900 and 1100 °C, which are the usual peak firing temperatures for bricks. The heating rate and cooling conditions were the same as for the series 1 test specimens.

Table 1
Chemical and mineralogical composition of clay IC.

	Content (wt%)
Oxide	
SiO_2	58.5 ± 0.3
Al_2O_3	20.2 ± 0.3
Fe_2O_3	7.14 ± 0.05
CaO	1.03 ± 0.04
MgO	1.56 ± 0.09
Na_2O	0.21 ± 0.03
K_2O	4.35 ± 0.09
LOI (1025 °C)	6.09 ± 0.08
Mineral	
Kaolinite	19 ± 2
Quartz	27 ± 1
Microcline	10 ± 1
Illite/muscovite	14 ± 2
Hematites	1 ± 0.5
Goethite	4 ± 0.5
Calcite	1 ± 0.5
Amorphous phase (mineral with low crystallinity)	24 ± 3

Dry and fired bulk density was determined by the mercury displacement method [15]. The mechanical strength of the fired pieces was determined by three-point bending in a mechanical testing machine (Instron 4507) with bar-shaped test pieces, 80 mm long, 20 mm wide, and 6 mm thick.

The thermal conductivity measurement tests were conducted according to an adapted experimental procedure of international standards ISO 8301:1991: Thermal insulation – Determination of steady-state thermal resistance and related properties – Heat flow meter apparatus, and ISO 8302:1991: Thermal insulation – Determination of steady-state thermal resistance and related properties – Guarded hot plate apparatus. These standards set out how to measure the thermal conductivity of parallelepiped test pieces by the Hot Guarded Plate method.

The phases present in the green and fired pieces were quantified by X-ray diffraction with the Rietveld method [16–18] using an internal standard [19,20] to quantify the amorphous phase. Fluorite was used as internal standard in a 5% (w/w).

A BRUKER Theta-Theta model D8 Advance diffractometer with CuKα radiation (λ = 1.54183 Å) was used. The generator settings were 45 kV and 30 mA. The XRD data were collected in a 2θ of 5–90° with a step width of 0.015° and a counting time of 1.2 s/step. A VÅNTEC-1 detector was used. In this study the 4.2 version of the Rietveld analysis program DIFFRACplus TOPAS was used, assuming a pseudo-Voight function to describe the peak shapes. This commercial software is supplied by BRUKER. The refinement protocol included the background, the scale factors and the global-instrument, lattice, profile and texture parameters. The basic approach is to get the best diffraction data, identify all the crystalline phases present and input basic structural data for all phases, then let the computer model the data until the best fit to the experimental pattern is obtained. The R_{WP} (R-weighted pattern) and GOF (goodness of fit) disagreement factors were registered.

Pore size distribution of fired samples was determined from the intrusion–extrusion curves obtained by mercury porosimetry (Micromeritic AutoPore IV). The porous texture of the polished test pieces was observed in a scanning electron microscope (Philips XL30).

3. Results

3.1. Influence of green porosity

Table 2 details the pressing pressure (P), firing temperature (T), dry bulk density (ρ_S), fired bulk density (ρ_C), degree of

Table 2
Characteristics of the series 1 test pieces.

P (MPa)	T (°C)	ρ_S (kg/m^3)	ρ_C (kg/m^3)	ζ	λ (W/m °C)	σ (MPa)
10	1000	1789 ± 2	1800 ± 2	0.006	0.49 ± 0.01	6.4 ± 0.9
16		1870 ± 2	1886 ± 2	0.008	0.52 ± 0.01	10.3 ± 0.4
25		1955 ± 2	1973 ± 2	0.009	0.56 ± 0.01	17.7 ± 0.4
60		2099 ± 3	2130 ± 3	0.015	0.61 ± 0.02	25 ± 3

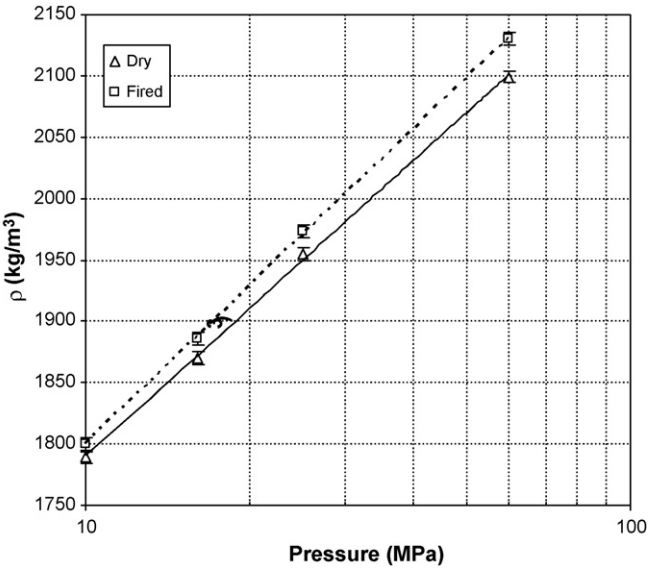

Fig. 1. Evolution of dry and fired bulk density with pressing pressure.

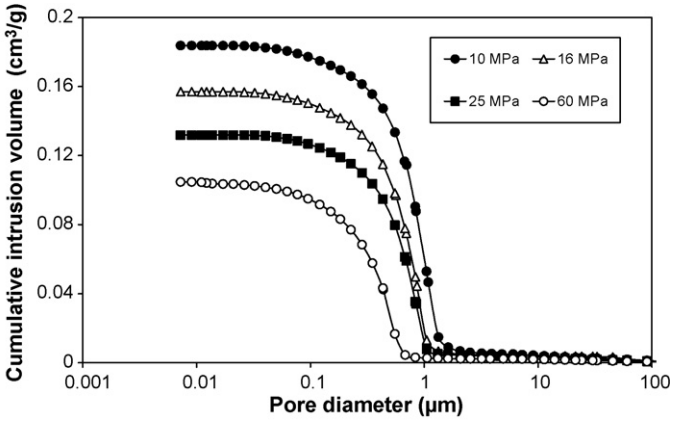

Fig. 2. Pore size distribution (mercury intrusion curves) of the 1000 °C fired test pieces.

sintering progress (ζ) defined according to Eq. (1), thermal conductivity (λ), and mechanical strength (σ) of the series 1 test pieces, in which pressing pressure was varied and peak firing temperature was kept steady.

$$\zeta = \frac{\rho_C - \rho_S}{\rho_S} \quad (1)$$

The variation of dry bulk density and fired bulk density as a function of pressing pressure is plotted in Fig. 1. It may be observed that the variation of dry bulk density with pressure follows a logarithmic trend, in accordance with the compaction mechanism proposed by Reed [21]. At the tested firing temperature, fired bulk density also follows the same trend, displaying very similar values to those of dry bulk density as a result of the scarce progress of the sintering process which, in this type of material (illitic–kaolinitic with quartz), occurs in the presence of liquid phase during firing at 1000 °C. At this temperature, the low linear shrinkage of the pieces (about 2.0%) only manages to offset the increase in porosity related to the decomposition of the clay minerals, calcite, and organic matter initially present in clay IC.

The phases present in the fired pieces formed at different pressures are listed in Table 3. The only detected crystalline phases were quartz, microcline, and hematites. Comparison with the corresponding values of the green pieces shows that, when these pieces were fired at 1000 °C, the quartz remained undissolved, the potassium feldspar partly fused, and the clay minerals fully dehydroxylated, increasing the amorphous phase content. In addition, the quantity of hematites increased owing to the disappearance of goethite. It may be concluded, therefore, that the pressing pressure does not influence the phases present in the test pieces fired at 1000 °C.

These results show that the variation of pressing pressure only affects the porosity of the fired piece. This series of experiments thus allows the variable 'porosity' to be isolated, in order to analyse its influence on thermal conductivity and fired mechanical strength.

Fig. 2 plots the mercury intrusion curves of series 1 fired test pieces. As pressing pressure increases porosity decreases (total cumulative intrusion volume diminishes) and the curves are shifted towards the left, i.e., the specimens have smaller pores. Pore size distribution becomes narrower as a consequence of eliminating the bigger pores [22] (associated to the larger particles such as quartz and microcline). Pressing pressure does not alter the smallest pores (associated with fine particles such as illite and kaolinite).

The variation of thermal conductivity as a function of fired bulk density is plotted in Fig. 3. The figure shows that, in the range of tested densities, there is a linear relationship between thermal conductivity and bulk density of the test pieces, such that when the bulk density of the pieces increases, thermal conductivity also rises. Since the firing temperature was kept constant in this series of test pieces, the phase composition also remained constant, while fired bulk density changed owing to the variation in pressing pressure. This relationship has been described in numerous studies and is attributed to the insulating effect of the pores in the pieces.

Table 3
Phases present (% by weight) and Rietveld disagreement factors (R_{WP} and GOF) in the series 1 fired test pieces.

P (MPa)	T (°C)	Quartz (%)	Microcline (%)	Hematites (%)	Amorphous phase (%)	R_{WP} (%)	GOF
10	1000	27 ± 1	9 ± 0.5	4 ± 0.5	63 ± 2	3.41	1.45
16		27 ± 1	8 ± 0.5	4 ± 0.5	64 ± 2	3.57	1.50
25		27 ± 1	9 ± 0.5	4 ± 0.5	64 ± 2	3.66	1.54
60		26 ± 1	9 ± 0.5	4 ± 0.5	65 ± 2	2.35	1.41

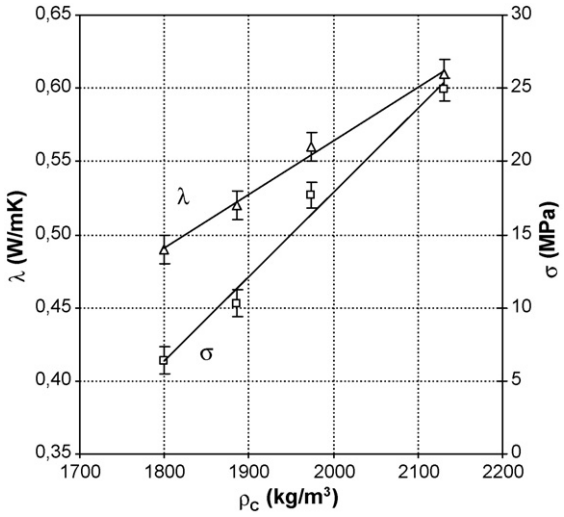

Fig. 3. Evolution of thermal conductivity (λ) and mechanical strength (σ) with bulk density (ρ_C) in the fired pieces. Series 1.

The slope of the resulting straight line is 3.66×10^{-4} W m^2/(kg K), which is close to the results obtained by other authors [3,7,8], who report values ranging from 3.6 to 4.4×10^{-4} W m^2/(kg K). However, this value is lower than the value specified in standard EN 1745, which establishes that the relation between thermal conductivity and bulk density in fired-clay products is 4.6×10^{-4} W m^2/(kg K). The scatter in the slope values provided by different authors requires the relationship between thermal conductivity and bulk density to be determined for each specific clay.

Fig. 3 also shows the variation of mechanical strength with fired bulk density. When the bulk density of the fired pieces increases (due to the increase of the pressing pressure), their mechanical strength is also observed to rise, owing to the lower porosity, smaller average pore size (Fig. 2) and, hence, greater interconnectivity between the solid phase in the pieces [23,24].

Fig. 4 (top) shows the scanning electron microscope photographs of a polished cross-section of the test piece pressed at 16 MPa and fired at 1000 °C. The black areas in the photograph correspond to pores, which surround identifiable feldspar and quartz particles (marked F and Q, respectively) with angular edges. These large particles, which have scarcely been integrated into the matrix, have not yet begun to fuse or to dissolve. It may be observed, furthermore, that the porous system is interconnected and that other, smaller, less well-defined particles (whose analysis shows that they consist of Si, Al, K, Fe, and O) lie between the quartz and the feldspar particles, indicating the presence of clay agglomerates. The test pieces pressed at 10 and 25 MPa exhibit the same appearance.

The test pieces formed at 60 MPa (Fig. 4, bottom) display a different appearance from the foregoing ones, notably a lower porosity, which means that there is a more continuous solid matrix than that in the test pieces pressed at lower pressures. The rise in pressing pressure eliminates the larger-sized pores, yielding denser pieces with a narrower pore size distribution. This microstructure favours sintering [25,26] and it undergoes a greater degree of densification when the quantity of liquid

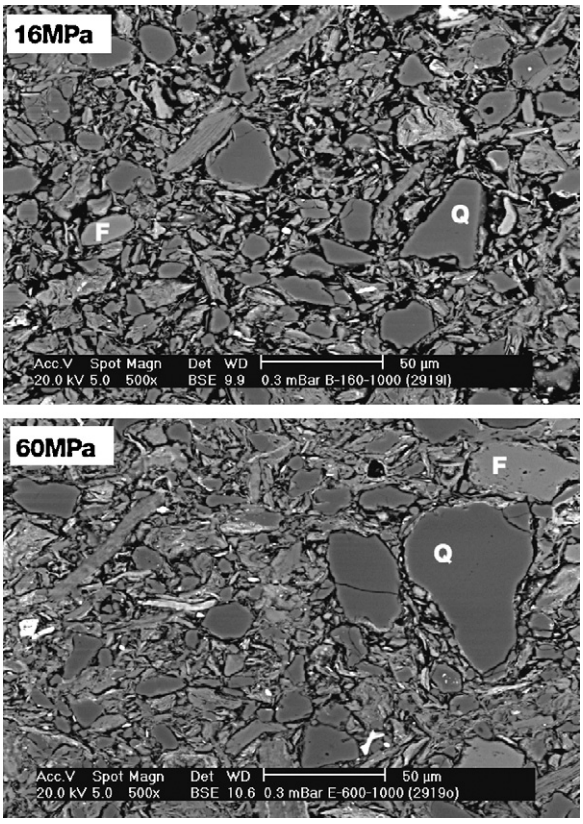

Fig. 4. Cross-section of the sample processed at T = 1000 °C. Top: P = 16 MPa, bottom: P = 60 MPa. Q: Quartz, F: Feldspar.

phase that forms is small, as occurs at the test temperature. This progress in the sintering process is also to be observed in the values of parameter ζ (Table 2).

3.2. Influence of the firing temperature

In this series of test pieces (series 2), dry porosity was kept constant and peak firing temperature was modified. The results are presented in Table 4.

Pore size distribution of fired pieces is shown in Fig. 5. Raising firing temperature produces a greater amount of liquid phase and a drop in liquid-phase viscosity. This enables eliminating pores, increasing shrinkage and lowering porosity. Liquid-phase sintering involves a gradual elimination of pores as the liquid phase forms. As temperature increases the curves progressively shift towards larger pore sizes, i.e., pores grow owing to the progressive removal of the smallest pores. Pore growth with temperature in initial and intermediate-stage sintering in the presence of liquid phase has been observed in clayey compositions [25] and glassy materials [26,27]. The phenomenon arises because the elimination of smaller pores produces differential shrinkage of the material, giving rise to growth of the larger pores. This coarsening is the result of heterogeneous pore sizes in the green packing.

The evolution of fired bulk density and thermal conductivity with firing temperature is plotted in Fig. 6. The figure shows that the fired bulk density of the pieces increases exponentially with firing temperature, in the tested firing temperature range.

Table 4
Characteristics of the series 2 test pieces.

P (MPa)	T (°C)	ρ_S (kg/m^3)	ρ_C (kg/m^3)	ζ	λ (W/m °C)	σ (MPa)
25	900	1955	1857 ± 2	−0.046	0.41 ± 0.01	7.3 ± 0.3
	940		1916 ± 2	−0.030	0.50 ± 0.01	13.3 ± 0.3
	1000		1973 ± 2	0.009	0.56 ± 0.01	17.7 ± 0.4
	1050		2108 ± 3	0.075	0.63 ± 0.02	23.3 ± 0.8
	1100		2341 ± 4	0.194	0.72 ± 0.02	37.5 ± 0.4

Table 5
Series 2. Phase composition (% by weight) and Rietveld disagreement factors (R_{WP} and GOF) of the fired pieces.

P (MPa)	T (°C)	Quartz (%)	Microcline (%)	Hematites (%)	Amorphous phase (%)	R_{WP} (%)	GOF
25	900	26 ± 1	10 ± 0.5	3 ± 0.5	61 ± 2	3.10	1.30
	940	27 ± 1	10 ± 0.5	3 ± 0.5	62 ± 2	3.15	1.30
	1000	27 ± 1	9 ± 0.5	4 ± 0.5	64 ± 2	3.43	1.42
	1050	26 ± 1	8 ± 0.5	4 ± 0.5	65 ± 2	3.52	1.49
	1100	25 ± 1	7 ± 0.5	5 ± 0.5	64 ± 2	3.66	1.54

This sintering progress is also observed in the values of parameter ζ, included in Table 4.

The thermal conductivity values are also plotted in Fig. 6. These do not vary analogously to those of fired bulk density, but display a linear variation with temperature. The fact that thermal conductivity does not vary linearly with fired bulk density, as occurred in series 1, is because in this case not only the porous texture is being modified but also the phases present in the fired pieces could change.

The phase contents in the test pieces fired at different temperatures are listed in Table 5. It shows that the quartz content does not change noticeably in the tested temperature range, though it should be noted that the quartz peak width increases at 1100 °C, indicating a certain quartz degradation, probably owing to the onset of quartz dissolution. Microcline decreases progressively to 5% at 1000 °C, and subsequently stabilises. These outcomes indicate that there are no important changes in crystalline phase type and content in the fired pieces, which is why the changes in thermal conductivity must be related to the change in the porous texture of the pieces, as a result of sintering progress.

Thermal conductivity is plotted versus bulk density of the series 2 test pieces (hollow symbols) and series 1 test pieces (solid symbols) in Fig. 7. It shows that thermal conductivity increases with bulk density in both series, though the relation is not linear in series 2. Thus, at low bulk densities (1900 kg/m^3), the increase in thermal conductivity is much more pronounced than at the highest bulk densities (2200 kg/m^3). Comparison with the results obtained for series 1 (solid symbols) shows that the curve slope of the series 2 pieces is higher in the first stretch ($\rho_C < 2000$ kg/m^3), whereas in the second stretch ($\rho_C > 2100$ kg/m^3), it is practically identical to that observed for the series 1 pieces. These findings indicate that thermal conductivity does not only depend on total porosity, but that there are also other factors, such as pore size distribution,

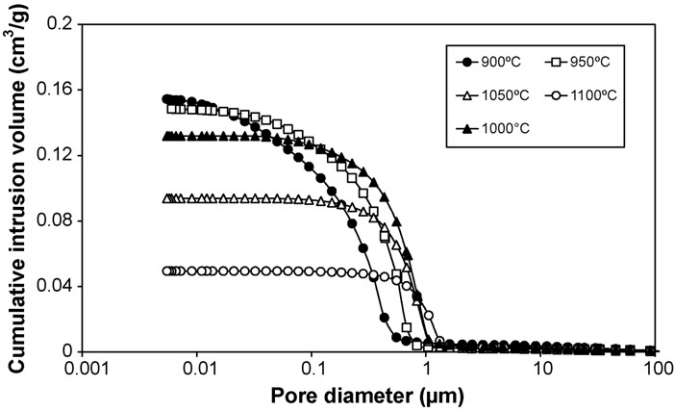

Fig. 5. Pore size distribution (mercury intrusion curves) of the series 2 fired test pieces.

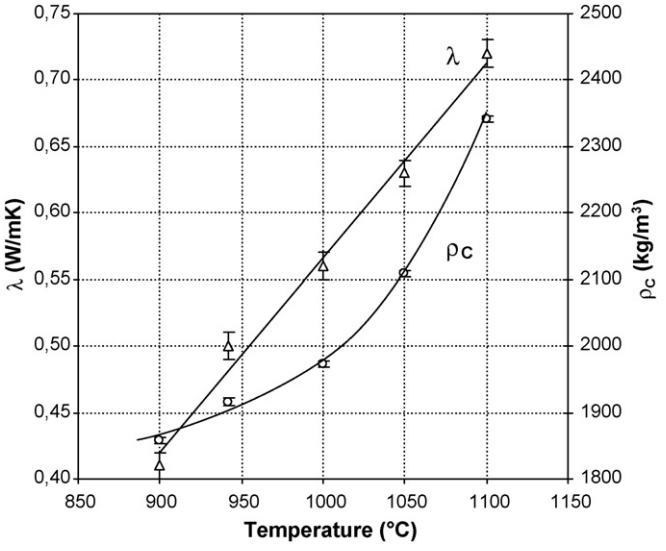

Fig. 6. Evolution of thermal conductivity (λ) and fired bulk density (ρ_C) with firing temperature.

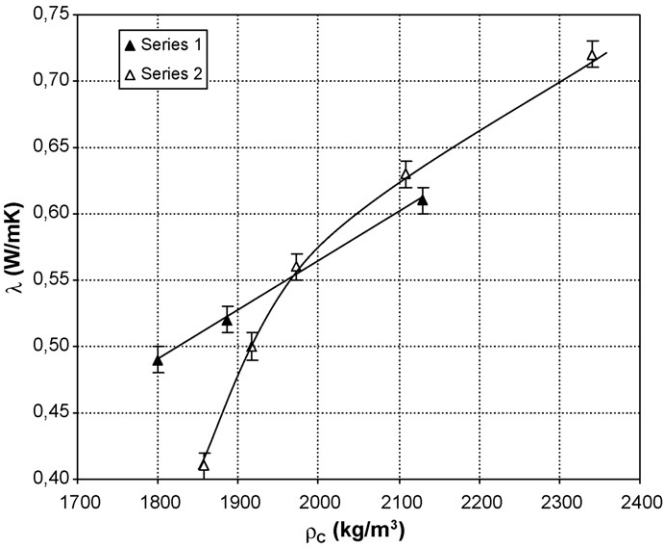

Fig. 7. Evolution of thermal conductivity (λ) with fired bulk density (ρ_C).

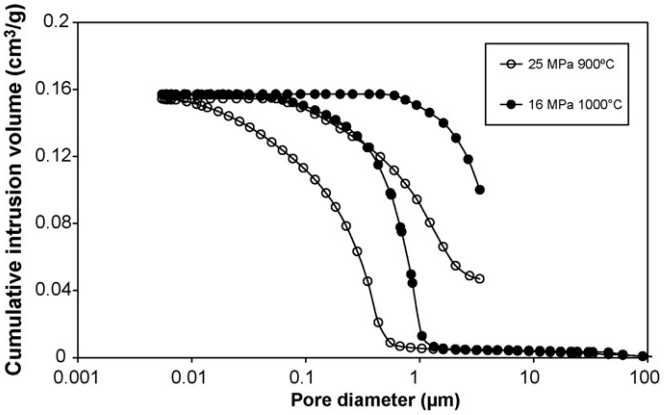

Fig. 8. Mercury intrusion–extrusion curves of test pieces with the same porosity.

which change significantly with temperature [25] and which determine the continuity of the solid phase.

The main difference between the two series of test pieces lies in the firing temperature. While in series 1, the changes in fired porosity are exclusively due to the variations in green porosity, and the quantity and composition of the phases present in the pieces remain constant, the changes in porosity in series 2 are mainly due to sintering progress. These two ways of reducing the porosity of the fired pieces (by either increasing green bulk density or firing temperature) significantly affect the porous texture of the pieces and, hence, their thermal conductivity.

Fig. 7 shows that thermal conductivity varies markedly with fired bulk density at low firing temperatures. It was verified, however, that the crystalline phases did not change significantly in the pieces, which is why thermal conductivity seems to depend solely on the porous texture of the pieces, which changes considerably at these temperatures [25]. Even though the density of some of the series 2 test pieces is the same as that of some series 1 test pieces, the porous texture will be different [22,28,29]. At low firing temperatures, when hardly any liquid has formed, small pores have not yet been eliminated in the piece, which is why these pores must provide the piece with a more insulating character. When the temperature rises and those pores are eliminated, the solid that contains them densifies, increasing the continuity of the solid and, hence, its thermal conductivity.

Fig. 8 plots the mercury intrusion–extrusion curves for test pieces with the same porosity but whose thermal conductivities are different, that is a test piece from the series 1 obtained at a pressure of 16 MPa and fired at 1000 °C and a series 2 test piece fired at 900 °C. On comparing the hysteresis between its corresponding intrusion–extrusion curves, it can be assessed that the amount of mercury expelled is bigger in the 900 °C test piece. The entrapment of mercury is primary due to the presence of bottle-necked pores [30] (the entrance opening to a pore is usually smaller than the actual cavity). Pore shape strongly influences the mercury extrusion behaviour [31], thus, a large amount of mercury trapped inside the pores could represent a higher tortuosity and lower degree of connectivity among them. On raising firing temperature, the initially interconnected porous system progressively loses connectivity as sintering advances and pores start closing, increasing the solid phase connectivity and, consequently, thermal conductivity.

In order to establish the evolution of the porous texture with temperature, polished cross-sections of the test pieces corresponding to series 2 (Fig. 9) were observed. The microstructure displays notable changes as firing temperature increases. Thus, at the lowest temperature (900 °C, Fig. 9, top), the clay matrix exhibits high porosity, with an interconnected pore system as a result of the scarce degree of sintering progress. The smallest pores had not yet been eliminated in this piece, these being customarily the pores that lie between the clay mineral particles. Large, irregular pores were observed (black areas in the photograph), corresponding to quartz and feldspar particles that were pulled out during sample polishing, confirming the poor integration of these particles in the matrix. At higher temperatures (1050 °C, Fig. 9, middle), liquid-phase formation begins to reduce significantly the porosity of the matrix, first eliminating the smallest pores and, as a result, increasing the size of the large ones. The matrix is denser and the continuity of the solid increases. Finally, at 1100 °C (Fig. 9, bottom), porosity has been significantly reduced, the piece is considerably denser and the largest pores remain uneliminated, these being isolated and displaying rounded edges owing to the arising liquid phase [25]. It may be observed, furthermore, that the largest particles are fully integrated in the matrix because of the abundant quantity of liquid phase. Although the amount of amorphous phase does not seem to change significantly with temperature according to XRD data, the change in amorphous phase nature (non-vitreous/vitreous) is big enough to alter the microstructure. At low temperatures a significant amount of amorphous phase other than vitreous phase is present in the sample whereas at 1100 °C almost all amorphous phase must be liquid/vitreous phase.

The porous texture of the pieces depends on the degree of firing attained, which is a function of the sample's miner-

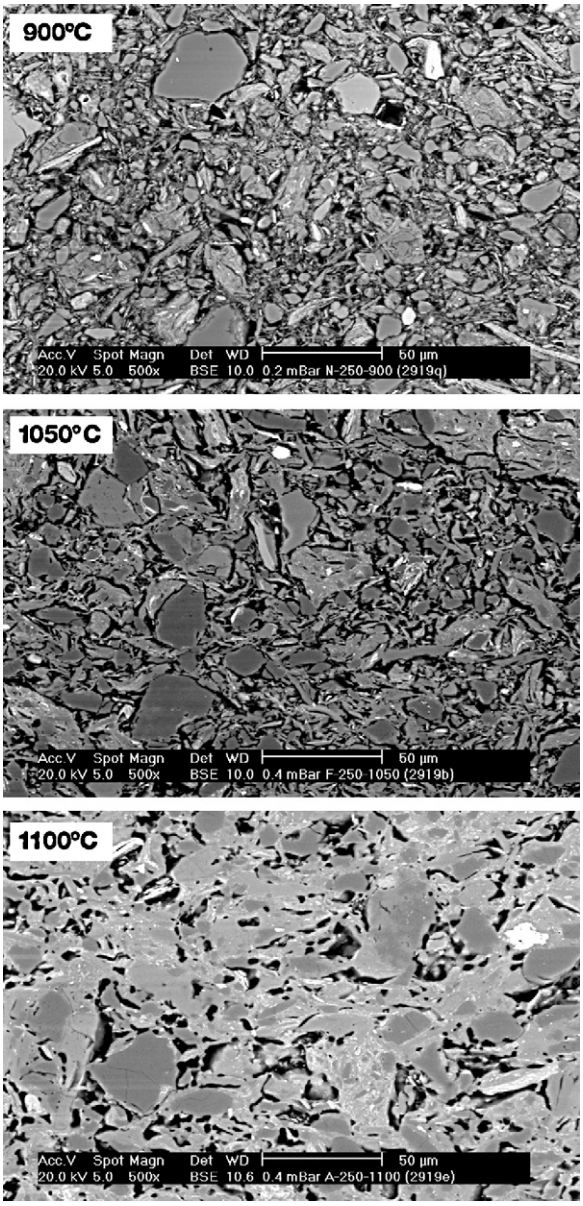

Fig. 9. Cross-section of the sample processed at $P = 25$ MPa. Top: $T = 900$ °C, middle: $T = 1050$ °C, bottom: $T = 1100$ °C.

alogical composition, its particle size, and the firing cycle used [25,28]. For the studied clay (IC), when firing was performed at temperatures of 1050 °C or higher, the thermal conductivity–fired bulk density pairs of values were observed to fit a straight line, while at lower temperatures there must be a relation at each of the tested temperatures as shown by the dashed lines in Fig. 10. This is due to the size of fine pores, which must remain constant at the same firing temperature. Liquid-phase viscosity is constant with T and determines the maximum pore size to be eliminated [26]. As a result, the solid phase connectivity depends on firing temperature. The variation of fired porosity in the series 1 test pieces is due to the decrease in large pores when pressing pressure is raised [22].

The evolution of mechanical strength with fired bulk density of the series 2 pieces follows a practically linear trend, as shown

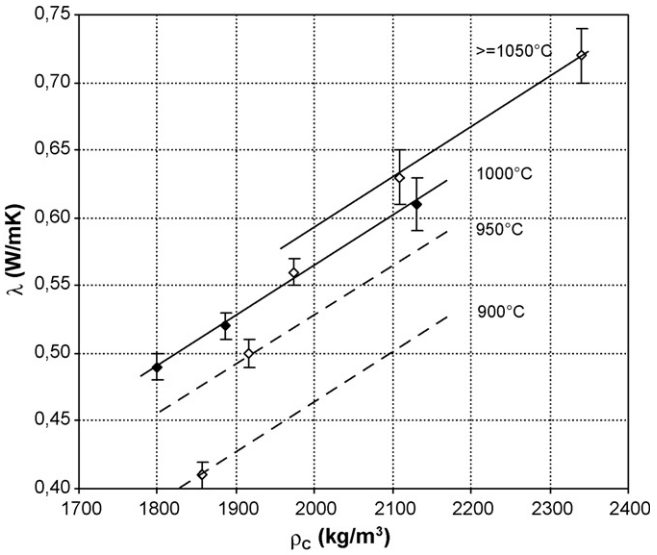

Fig. 10. Relation between thermal conductivity (λ) and fired bulk density (ρ_C).

in Fig. 11. The series 1 values also fit the same straight line, which indicates that the procedure used to obtain a given fired bulk density (by either increasing pressure or firing temperature) does not appear to influence the resulting mechanical strength. These results are in contrast to those displayed by thermal conductivity (Fig. 7), which evidences the lower thermal conductivity of the test pieces processed at low firing temperatures. The different effects of the tested process variables (pressing pressure and firing temperature) on mechanical strength and on thermal conductivity allow pieces to be obtained with low thermal conductivity and appropriate mechanical strength.

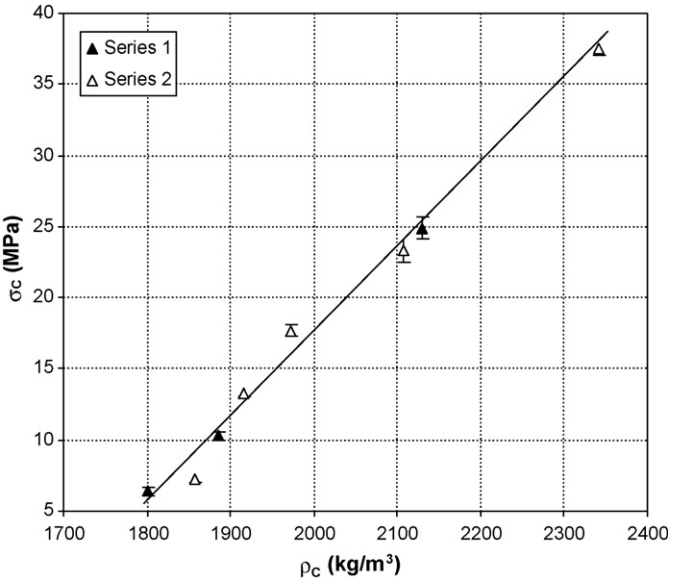

Fig. 11. Evolution of mechanical strength (σ) with bulk density (ρ_C) in the fired pieces.

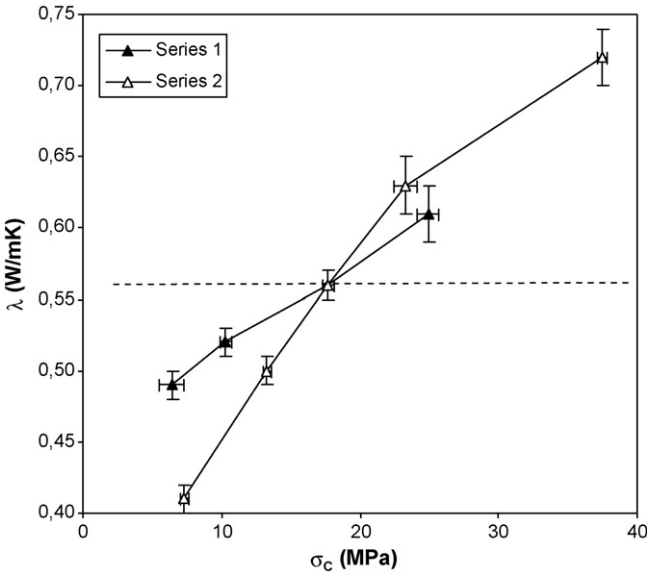

Fig. 12. Relation between thermal conductivity (λ) and mechanical strength (σ).

3.3. Relation between thermal conductivity and mechanical strength

One of the most effective ways of lowering the thermal conductivity of traditional ceramic products is by raising their porosity, for which different lightening additives are typically used that act on green porosity (low-density raw materials) or fired porosity (materials that burn out during firing). One of the disadvantages resulting from this approach is the impairment of the mechanical properties of products that sometimes have structural roles in buildings. This part of the study analyses the convenience of either decreasing the thermal conductivity of the pieces, by raising green porosity, or reducing their degree of firing. The former case leads to an effect resembling that obtained when organic additives are used that burn out during the firing stage.

The mechanical strength–thermal conductivity pairs of values for the two series of tested pieces are plotted in Fig. 12. It shows that thermal conductivity increases with mechanical strength, because both characteristics depend on the porous texture of the pieces. However, the slope of the two series of test pieces differs. The curves corresponding to both series intersect for the test piece formed at 25 MPa and fired a 1000 °C. A dashed line has been drawn through that point.

The results indicate that thermal conductivity can be reduced by lowering the forming pressure and/or the firing temperature. For the studied clay, processed under standard conditions (25 MPa and 1000 °C), it would be more convenient to decrease thermal conductivity by acting upon the firing temperature, since that would not cause such a great impairment of mechanical properties as that observed when the forming pressure was lowered. The foregoing assessment is based on the two studied properties (thermal conductivity and mechanical strength), though other aspects, such as moisture expansion of the ceramic product (which increases as firing temperature decreases), also need to be taken into account.

4. Conclusions

This study examines the influence that dry bulk density and firing temperature have on the thermal conductivity and mechanical strength of pieces made from a red-firing clay customarily used in the manufacture of traditional ceramic materials.

It was observed that, for the same material, thermal conductivity did not solely depend on the total porosity of the fired pieces, but that pore size distribution and pore interconnectivity need to be considered, which depend on the degree of firing attained and may also be influenced by the phases present in the pieces, whose content and/or composition could vary with firing temperature.

For the studied clay, the variation of thermal conductivity with total porosity followed the expected trend when the firing temperature was above 1000 °C. At lower firing temperatures, the variation was more pronounced due to the minor degree of densification, which meant that the piece still contained an important small pore fraction.

Thermal conductivity can be reduced in this type of material by increasing green porosity (or by adding organic lighteners) and/or lowering the firing temperature. Which of these two variables it is more advisable to modify should be studied on a case-by-case basis, in order not to reduce mechanical strength excessively.

Acknowledgments

This study has been funded by the Spanish Ministry of Education and Science within the frame of the National Plan for Scientific Research, Development and Technological Innovation 2004–2007, reference BIA2006-14242, through the European Fund for Regional Development (FEDER).

References

[1] M. Dondi, F. Mazzanti, P. Principi, M. Raimondo, G. Zanarini, Thermal conductivity of clay bricks: the influence of microstructure and phase composition, in: P. Vincenzini, M. Dondi (Eds.), Techna Science for New Technology of Silicate Ceramics, Techna, Faenza, 2003, pp. 223–230.
[2] M.M. Akiyochi, R. Pereira, A.P. da Silva, V. Pandolfelli, Effect of alumina content, porosity and temperature on the thermal conductivity of refractories, Am. Ceram. Soc. Bull. 82 (6) (2003) 29–33.
[3] A. Erker, The thermal conductivity of the brick ceramic body. Part 1, Zi. Int. 55 (10) (2002) 34–42.
[4] E.K. Jungk, W. Krcmar, B. Linner, Reduction of the thermal conductivity on clay masonry units by optimization of the ceramic body structure, Zi. Int. 49 (6) (1996) 368–376.
[5] E.K. Jungk, H. Halseband, K. Ebert, W. Kromar, Porosifiers for the production of lightweight tricks, Tile Brick Int. 13 (1) (1997) 7–12.
[6] J. García-Ten, G. Silva, V. Cantavella, M. Lorente, Utilización de materiales aligerantes en la fabricación de bloques de Termoarcilla. Influencia sobre la conductividad térmica y el comportamiento en el proceso, Conarquitectura 16 (2005) 89–96.
[7] E. Rimpel, S.M. El Ghazzali, Influence of the mineral constituents and equilibrium moisture on the thermal conductivity of bricks, in: Zi-Annual: Annual for the Brick and Tile, Structural Ceramics and Clay Pipe Industries, Bauverlag, Wiesbaden, (1998), pp. 28–52.
[8] D. Hauck, M. Ruppik, S. Hörnschemeyer, F. Richter, B. Henschker, Influence of the raw material composition on the strength and thermal

conductivity of vertically perforated clay bricks and blocks, in: Zi-Annual: Annual for the Brick and Tile, Structural Ceramics and Clay Pipe Industries, Bauverlag, Wiesbaden, (1998), pp. 54–79.
[9] A. Erker, The thermal conductivity of the brick ceramic body. Part 2, Zi. Int. 55 (11) (2002) 32–37.
[10] N.H. Abu-Hamdeh, R.C. Reeder, Soil thermal conductivity: effects of density, moisture, salt concentration, and organic matter, J. Soil Sci. Soc. Am. 64 (2000) 1285–1290.
[11] M. Dondi, P. Principi, M. Raimondo, G. Zanarini, The thermal conductivity of bricks produces with Italian clays, L'ind. Laterizio 65 (2000) 309–320.
[12] M. Sveda, New look at mathematical relationships among physical properties of brick products, Br. Ceram. Trans. 99 (4) (2000) 181–186.
[13] M. Sveda, Influence of calcium carbonate on the physical properties of a clay body: Part 2, Zi. Int. 53 (4) (2000) 30–35.
[14] W. Schulle, J. Kutzendörfer, Relationship of thermal conductivity and strength to the mean pore diameter in chamotte lightweight refractory blocks, Zi. Int. 41 (6) (1988) 300–303.
[15] J.L. Amorós, A. Blasco, T. Manfredini, P. Pozzi, A new experimental method for measuring apparent density in ceramics: aspects of technique and applications, Ind. Ceram. 7 (4) (1987) 200–204.
[16] R.A. Young (Ed.), The Rietveld Method, University Press, Oxford, 1996.
[17] A.L. Ortiz, F. Sánchez-Bajo, N.P. Padture, F.L. Cumbrera, F. Guiverteau, Quantitative polytype-composition análisis of SiC using X-ray diffraction: a critical comparación between the polymorphic and the Rietveld method, J. Eur. Ceram. Soc. 21 (2001) 1237–1248.
[18] A.H. De Aza, A.G. De La Torre, M.A.G. Aranda, F. José Valle, S. De Aza, Rietveld quantitative analysis of Buen Retiro porcelains, J. Am. Ceram. Soc. 87 (3) (2004) 449–454.
[19] A.G. De La Torre, S. Bruque, M.A.G. Aranda, Rietveld quantitative amorphous content analysis, J. Appl. Crystal. 34 (2) (2001) 196–202.
[20] J. Martín-Márquez, A.G. De la Torre, M.A.G. Aranda, J.M. Rincón, M. Romero, Evolution with temperature of crystalline and amorphous phases in porcelain stoneware, J. Am. Ceram. Soc. 92 (1) (2009) 229–234.
[21] J.S. Reed, Principles of Ceramics Processing, 2nd ed., John Wiley, New York, 1995.
[22] J.L. Amorós, V. Beltrán, A. Escardino, M.J. Orts, Permeabilidad al aire de soportes cocidos de pavimento cerámico. I. Influencia de las variables de prensado y de la temperatura de cocción, Bol. Soc. Esp. Ceram. Vidr. 31 (1) (1992) 33–38.
[23] J.L. Amorós, C. Felíu, F. Ginés, J.V. Agramunt, Mechanical strength and microstructure of green ceramic bodies, Ceram. Acta 8 (6) (1996) 5–19.
[24] J.L. Amorós, V. Cantavella, J.C. Jarque, C. Felíu, Green strength testing of pressed compacts: an analysis of the different methods, J. Eur. Ceram. Soc. 28 (4) (2008) 701–710.
[25] M.J. Orts, A. Escardino, J.L. Amorós, F. Negre, Microstructural changes during the firing of stoneware floor tiles, Appl. Clay Sci. 8 (2–3) (1993) 193–205.
[26] M.D. Sacks, T.Y. Tseng, Preparation of SiO_2 glass from model powder compacts. Part 2: Sintering, J. Am. Ceram. Soc. 67 (8) (1984) 532–537.
[27] M.D. Sacks, T.Y. Tseng, Preparation of SiO_2 glass from model powder compacts. Part 3: Enhanced densification by sol infiltration, J. Am. Ceram. Soc. 71 (4) (1988) 245–249.
[28] J.L. Amorós, M.J. Orts, J. García-Ten, A. Gozalbo, E. Sánchez, Effect of green porous texture on porcelain tile properties, J. Eur. Ceram. Soc. 27 (5) (2007) 2295–2301.
[29] M.J. Orts Tarí, Sinterización de piezas de pavimento gresificado, Doctoral dissertation, Universitat de València, Chemical Engineering Department, Castellón, 1991.
[30] P.A. Webb, C. Orr, Analytical Methods in Fine Particle Technology, Micromeritics Instrument Corporation, Norcross, GA, 1997.
[31] F. Schüth, K.S.W. Sing, J. Weitkamp (Eds.), Handbook of Porous Solids, Wiley-VCH Verlag GmbH, Germany, 2002.

Francisco Javier García Ten graduated in chemistry from the University of Valencia, Spain, in 1987. He earned the PhD in chemistry from the University Jaume I in 2005. Since 1989 he is doing his research activity at the Instituto de Tecnología Cerámica, as senior researcher. He is also assistant professor of chemical engineering at the University Jaume I of Castellón since 1996. He has co-authored over 50 scientific/technical papers, presented more than 60 communications at conferences and scientific/technical meetings, is co-inventor of 2 patents and co-author of 4 books or monographs in the field of ceramic technology. He has participated as senior researcher in over 60 R&D and Technology Consultancy projects conducted at the Instituto de Tecnología Cerámica, funded by ceramic tile manufacturers, frit and glaze producers, machinery builders for the ceramic industry, brick and roofing tile manufacturers, etc., as well as by public bodies belonging to the Valencia Regional Government, Spanish Government and European Union.